Detection of heroin addiction- and relapse-induced axonal transport dysfunction in the brain in vivo by MRI

Jun Yang (imdyang@qq.com)
The Third Affiliated Hospital of Kunming Medical University: Yunnan Cancer Hospital
https://orcid.org/0000-0002-1943-3979

Yueyuan Luo
The Third Affiliated Hospital of Kunming Medical University: Yunnan Cancer Hospital

Chengde Liao
The Third Affiliated Hospital of Kunming Medical University: Yunnan Cancer Hospital

Long Chen
The Third Affiliated Hospital of Kunming Medical University: Yunnan Cancer Hospital

Yongjin Zhang
Kunming Medical University First Affilliated Hospital

Shasha Bao
The Third Affiliated Hospital of Kunming Medical University: Yunnan Cancer Hospital

Ailin Deng
The Third Affiliated Hospital of Kunming Medical University: Yunnan Cancer Hospital

Tengfei Ke
The Third Affiliated Hospital of Kunming Medical University: Yunnan Cancer Hospital

Qinqing Li
The Third Affiliated Hospital of Kunming Medical University: Yunnan Cancer Hospital

Research Article

Keywords: heroin, addiction, relapse, axonal transport, manganese, magnetic resonance imaging, olfactory pathway

Posted Date: February 1st, 2022

DOI: https://doi.org/10.21203/rs.3.rs-1280587/v1

Abstract

Purpose Heroin is a highly addictive drug that causes axonal damage. Here, manganese-enhanced magnetic resonance imaging (MEMRI) was used to dynamically monitor axonal transport in different stages after heroin addiction.

Methods Rodent models of heroin addiction (HA) and heroin relapse (HR) were established by injection of different doses of heroin solution at different times. Heroin-induced learning and memory deficits were evaluated by the Morris water maze (MWM). MEMRI was used to dynamically evaluate axonal transport through the olfactory pathway. The expression of proteins related to axonal structure and function were assessed by western blotting. Transmission electron microscopy (TEM) was used to observe ultrastructural changes. Neurofilament heavy chain (NF-H) protein levels were analyzed by immunofluorescence staining.

Result HA model rats and especially HR model rats showed worse spatial learning and memory abilities than control rats. Compared with HA model rats and control rats, HR model rats exhibited a significant increase in escape latency and significant decreases in the number of platform location crossings and time spent in the target quadrant. Mn^{2+} transport was accelerated in HA model rats. HR model rats exhibited a severely insufficient capacity for Mn^{2+} transport, and the axonal transport rate (ATR) was significantly reduced in these rats compared to control rats (P<0.001). The levels of cytoplasmic dynein and KIF5 in rats in the HR group were significantly decreased (P<0.001), and the levels of energy-related proteins, including COX IV and ATPB, were lower in the HR group than the control group (P<0.001). The brains of heroin-exposed rats showed an abnormal ultrastructure, exhibiting neuronal apoptosis and mitochondrial dysfunction. Heroin decreased the expression of NF-H, with the staining intensity being significantly reduced in tissues from HA and HR model rats (P<0.05).

Conclusion MEMRI can detect axonal transport dysfunction caused by long-term repeated exposure to heroin, and decreases in the levels of motor proteins and mitochondrial dysfunction may be the main causes of this axonal transport impairment. Thus, the study shows that MEMRI is a potential tool for visualizing axonal transport in individuals experiencing drug addiction, providing a new direction for the evaluation of addictive drug withdrawal.

Introduction

Drug abuse is currently one of the most serious public health and social problems worldwide. Heroin is the most commonly abused opiate (Büttner et al. 2000) and its use quickly leads to addiction. Addiction greatly impacts an individual's physical and mental health, moreover, it is difficult for individuals to quit using heroin, and relapse occurs easily. Long-term heroin exposure can cause damage to all body systems, the most critical of which is the nervous system, as injury to the nervous system results in irreversible brain damage(Gardini et al. 2012; Kumar et al. 2015). This brain damage can further aggravate dependence and contribute to relapse(Cadet et al. 2014). Moreover, cognitive impairment is a

common consequence of long-term heroin exposure(Ma et al. 2015). Studies have revealed that heroin abusers experience several cognitive disorders, including learning, memory, and executive function deficits(Gruber et al. 2007). Cognitive impairment not only causes an impulse to consume drugs, further increasing an individual's inability to stop taking drugs(Ornstein et al. 2000), but also increases the cost of clinical treatment because the resulting cognitive deficits lead to the need for additional rehabilitation.

Studies have shown that drug abuse can lead to cognitive impairment similar to that observed in Alzheimer's disease(Bassiony et al. 2017; Fitzpatrick et al. 2020; Kousik et al. 2014; Potvin et al. 2018). Increasing evidence suggests that cognitive impairment resulting from neurodegenerative disorders is closely related to impairment of axonal transport (W. Guo et al. 2020; Mandal et al. 2019; Martínez-Mármol et al. 2019; Sau et al. 2011). Notably, axonal degeneration is the main pathological feature of brain injury(Kashyap et al. 2020). Barnett et al reported that heroin addiction and heroin relapse can cause axonal damage(Barnett et al. 2001). Striking vacuolization of the cerebellar white matter, a decrease in the number of oligodendrocytes and axonal degeneration were observed upon neuropathological examination of inhaled heroin abusers (Sempere et al. 1991). Recently, Bora et al (Bora et al. 2012) also reported that the reduction in the axial diffusion rate of the longitudinal tract and right frontal white matter in users who have abused opioids for a long time may be related to axonal damage in these areas. Heroin addiction may lead to hyperphosphorylated tau protein deposition and neuroinflammation in the brain(Anthony et al. 2010; Büttner et al. 2006), further leading to neurodegenerative diseases(T. Guo et al. 2017). However, the mechanisms by which both addiction and relapse disrupt axonal transport, leading to cognitive deficits, have not been fully elucidated. Therefore, elucidating the mechanism underlying axonal transport defects in subjects with heroin addiction and individuals undergoing heroin relapse is essential for the development of new drug withdrawal strategies and cognitive rehabilitation methods.

Most methods used to assess axonal transport usually require animals to be euthanized and cannot provide in vivo research. Hence, a noninvasive method for evaluating axonal transport is needed. Although traditional functional magnetic resonance imaging (MRI) allows in vivo analysis, its ability to detect dynamic transmission is limited. Manganese-enhanced magnetic resonance imaging (MEMRI) has been proven to be a valuable method for noninvasive assessment of axonal transport in vivo(Almeida-Corrêa et al. 2018; Uselman et al. 2020; Yang et al. 2020). The mechanism behind MEMRI involves the ability of Mn^{2+}, a paramagnetic substance, to shorten the T1 relaxation time, making it to appear as a strong signal in T1-weighted (T1W) images(Lin et al. 1997). In addition, Mn^{2+} is a calcium analog. It can enter neurons through voltage-gated calcium channels(Silva et al. 2008). After being taken up by cells, Mn^{2+} is transported along neurons through microtubule-dependent axonal transport and reaches secondary neurons through transsynaptic transport(Deng et al. 2019; Pautler et al. 1998). Here, we used this imaging technique to observe the effects of long-term heroin exposure on axonal transport in rats.

In this study, we established rat models of heroin addiction and relapsed and used MEMRI to study heroin-induced changes in axonal transport; moreover, we conducted behavioral experiments to

investigate the cognitive function of these rats. Furthermore, the mechanism of axonal transport dysfunction was investigated.

Materials And Methods

1. Animals

All animal experiments were conducted in accordance with the standard guidelines of the Institutional Animal Care and Experiment Committee of our university. Adult male Sprague–Dawley rats (180-200 g) were used for the experiments. The rats were housed five per cage under a 12 h light-dark cycle (lights on at 7 am) in a temperature-controlled room (20 ± 4°C) and provided free access to water and food.

After the rats were allowed to adapt to laboratory conditions for 1 week, the rats were randomly allocated to 4 groups (n=15/group): the acute heroin exposure (AHE) group, heroin-addicted (HA) group, heroin relapsed (HR) group and control group.

2. Experimental design and treatments

Heroin (provided by the Narcotics Control Bureau, Department of Public Security, Yunnan) was dissolved in normal saline (0.9%). The heroin solution was injected into the rats intraperitoneally twice a day (9 am and 5 pm), and the dose used was chosen according to published study(Li, Xia, Li, Yin, & Liang 2017). The rats were injected with heroin solution at a dose of 3 mg/kg on the first day. The rats were intraperitoneally injected with heroin daily for 9 days, with the dose being increased by 3 mg/kg each day until a maximum dose of 27 mg/kg was reached on day 9. After peak exposure, heroin injections were ceased for a total of 10 days to allow natural withdrawal and detoxification. The period of heroin injection followed by spontaneous withdrawal was called the experimental stage.

Rats in the AHE group were injected with heroin for only one day. Rats in the HA group was subjected to three exposure addiction to detoxification cycles, and rats in the HR group were subjected to six cycles (Fig. 1). The dosage and frequency of administration during each stage were kept the same for rats in the HA and HR groups. Rats in the control group were injected with saline according to the same procedure.

3. Weight measurement and behavioral analysis

On day 9, 2 h after injection of heroin, abstinence symptoms were induced by intraperitoneal injection of 4 mg/kg naloxone hydrochloride (Marklin, Shanghai, #N822820), and the rats were observed for half an hour(Wu et al. 2015). The symptoms that were observed within 30 minutes, including jumping, rearing, writhing, shaking like a wet dog and teeth chattering teeth, were recorded, and successful establishment of the model was confirmed by referring to existing withdrawal symptom scoring standards(Pu et al. 2015). All rats were weighed every day prior to heroin administration, and the average body weight of the rats at each stage was calculated to evaluate the influence of heroin on body weight.

4. Morris water maze (MWM) test

The MWM test was used to study the cognitive function of the animals. The test was performed as described in previous studies(Barnhart et al. 2015; Lwin et al. 2021). The first test was performed to examine the spatial learning ability of the rats. The MWM apparatus consisted of a pool (a water tank) that was painted black and divided into four virtual quadrants. The pool was 150 cm in diameter and 70 cm high and filled with water to a depth of 50 cm; the temperature of the water was maintained at 23 ± 1°C. The test was performed in a dimly lit room, and a camera was placed directly above the center of the pool to track the movement of the animals in the pool. Each rat was subjected to four trials in which they were allowed to search for a submerged platform for a maximum of 60 s. If a rat found the platform, it was allowed to stay there for 10-15 s. If a rat did not find the platform within 60 s, it was guided to the platform by the investigator and kept there for 15-20 s. This procedure was performed four times a day with a 1-minute intertrial interval for five consecutive days. The average escape latency (time to reach the hidden platform) of the rats was recorded and taken as a measure of spatial learning.

On the sixth day, the spatial probe trial was performed to assess spatial memory. In this test, which involved a single session, the platform was removed from the tank, and the rats were placed in the pool in random quadrants of. Each rat was allowed to swim freely for 60 s. The tracking system recorded the time that each rat spent in the target area and the number of platform location crossings as measurements of spatial memory.

5. Magnetic resonance imaging (MRI)

After the MWM test, the rats were subjected to MRI. Nasal cavity perfusion was performed before MRI scans were acquired. The animals were anesthetized with 4% isoflurane mixed in 5 L/min air and 1 L/min O_2 for 5 minutes. Manganese chloride ($MnCl_2$) solution was administered intranasally. A nasal lavage of 10 μL of isotonic $MnCl_2$ solution (50 mM) was administered via the left nostril using a microsyringe (RWD Life Science CO, Shenzhen, #790001), and the animals were then returned to their cages. MEMRI scans were acquired with a 3T MRI system (Philips Ingenia, Netherlands) configured with an eight-channel phased-array animal coil (50 mm; Chenguang, Shanghai); scans were performed 6 and 24 h after $MnCl_2$ administration. Anesthetized animals were fixed in a device, and T1W images in the coronal plane were acquired using a turbo spin echo sequence with the following parameters: repetition time (TR) = 510 ms, echo time (TE) = 25 ms, number of signal averages (NSA) = 12, field of view 50 mm × 50 mm, matrix size 200 × 198, and slice thickness 1.2 mm. The acquisition duration was 11 minutes 01 s.

6. MEMRI analysis

The MRI data were analyzed using software on a multifunctional workstation (Syngo.via, version VB10B, Siemens, Erlangen, Germany). Regions of interest (ROIs) were manually drawn on the ipsilateral and contralateral sides, including in the olfactory bulb (OB), proximal olfactory tract (POT) and distal olfactory tract (DOT) and muscle (MS), and signal intensity (SI) values of $MnCl_2$ solution were obtained at each time point. The ROIs were located in the center of each area and were of the same size and shape. Standardized with the mean signal of the ipsilateral muscle in the same slice. The enhanced intensity of Mn^{2+} in the ROIs was calculated by the following formula: $SI = S_{Mn(ip)} - S_{Mn(con)} / S_{MS}$, where $S_{Mn(ip)}$,

$S_{Mn(con)}$ and S_{MS} indicate the signal intensity (SI) in the Mn^{2+} enhancement area and the corresponding location on the contralateral side and the SI in the ROI in ipsilateral muscle (MS) respectively. The axonal transport rate (ATR) of Mn^{2+} was estimated according to the change in SI between two time points and calculated as follows: $(SI_{24h} - SI_{6h})$/time. Fig. 2 shows the method used to measure the SI.

7. Western blotting

Following MEMRI, six rats from each group were euthanized with 10% chloral hydrate, and fresh olfactory bulb and prefrontal lobe tissues were removed. After protein was extracted, the protein content was measured by the bicinchoninic acid (BCA) method. A sodium dodecyl sulfate–polyacrylamide gel electrophoresis (SDS–PAGE) gel was prepared, and the protein samples were subjected to electrophoresis and transferred onto a polyvinylidene fluoride (PVDF) membrane. The membrane was incubated with 5% skim milk and then incubated overnight at 4°C with the following primary antibodies: anti-cytoplasmic dynein (Abcam, #ab170947, 1:1000), anti-ATPB (Abcam, #ab170947, 1:10000), anti-COX IV (Cell Signaling, #4850, 1:1000), anti-KIF5A + KIF5B + KIF5C (Abcam, #ab62104, 1:1000) and anti-β-actin (Abmart, #P30002, 1:1000). After washing with Tris-buffered saline (TBST), the membrane was incubated with secondary antibody working solution for 60 minutes. After three washes, chemiluminescence was used for detection and image collection. ImageJ software (https://imagej.nih.gov/) was used to analyze the photos.

8. Transmission electron microscopy (TEM)

OB tissues from rats in the HR and control groups were analyzed by TEM (n=3 per group). Fresh tissues were cut into small 1 mm^3 pieces and fixed overnight in 2.5% glutaraldehyde solution. Then, the tissues were further fixed in 1% osmium tetroxide for 2 h before being dehydrated in gradient ethanol solutions, embedded in epoxy resin, sliced into ultrathin sections with a microtome, double stained with uranyl acetate and lead citrate, and observed and photographed under a transmission electron microscope (JEM-1400FLASH, Japan Electronics).

9. Immunofluorescence

After the rats were euthanized, they were perfused through the heart with sodium phosphate buffer containing 4% paraformaldehyde (PFA), and the appropriate brain tissues were removed. The paraffin-embedded brain tissues were cut into 5 mm sections and then incubated for 30 minutes in a peroxidase sealant containing 3% H_2O_2. After washing with phosphate-buffered saline (PBS), the sections were blocked in bovine serum albumin for 30 minutes. Then, the sections were incubated with a neurofilament heavy chain (NF-H) antibody (1:200, Biolegend, #835801) overnight at 4°C. After washing, the sections were incubated with biotinylated secondary antibody. Finally, under a fluorescence microscope, the number of positive cells in each slide was counted, and the average fluorescence intensity was calculated.

10. Statistical analysis

All data are presented as the means ± standard errors of the mean (SEM). Student's t test was used to analyze the significance of the differences between rats from the two groups. The escape latency data for the four groups obtained during the water maze training trials were analyzed by two-way analysis of variance (ANOVA). A nonparametric test was used if the data did not meet the requirements for a normal distribution. The Pearson method was used for correlation analysis. The experimental data were analyzed and images were made with SPSS 22.0 software and Origin 18.0 software. $P<0.05$ was considered statistically significant.

Results

1. Withdrawal scores and weight

The success of model establishment was assessed according to the reaction of the rats after naloxone administration. The withdrawal score of HA model rats was 12.16±1.47 and that of HR model rats was 13.66±0.81; both of these values were significantly higher than the withdrawal score of rats in the control group (2.5±0.83) ($P<0.001$), indicating the successful establishment of a physiological heroin dependence model. In addition, the score of HR model rats was higher than that of HA model rats, and the difference was significant ($P<0.05$, Fig. 3).

Heroin decreased body weight to different degrees. At the end of the observation period, the average weight of the HA model rats was 294.4±4.5 g, which was significantly lower than that of rats in the control group, i.e., 333.3±4.8 g ($P<0.001$). Weight loss was more obvious in HR model rats; the weight of rats in the HR group was 186.56±4 g, while the weight of rats in the control group increased to 449.5±2 g ($P<0.001$). Additionally, beginning in the third cycle of heroin abuse, the weight loss of heroin-exposed rats began to gradually increase. Compared with that of rats in the control group, the weight of HA model rats decreased by 11%, and the weight of the HR model rats decreased by 16%. In the 6th cycle, the weight of HR model rats was severely reduced, as it was 57% lower than that of rats in the control group, as shown in Fig. 4.

2. MWM test

2.1 Spatial learning

In the training trials, heroin had a significant effect on escape latency. As training continued, the escape latency of HA and HR model rats gradually decreased. On the first day of training, there was no difference in escape latency between rats in the different groups ($P>0.05$). The escape latency of HA and HR model rats was longer than that of control rats from the second day to the end of the training period. The escape latency of rats in the HR group was longer than that of rats in the HA group ($P<0.001$). The data showed that heroin exposure had a significant impact on the spatial learning ability of rats and that this effect was more severe in HR model rats than in HA model rats. Swimming speed was not significantly different between rats in the heroin-exposed groups ($P>0.05$), as shown in Fig. 5.

2.2 Spatial memory

After the last day of the training phase, we performed a probe test and analyzed the time that the rats spent in the target quadrant zone and the number of times the rats crossed the previous platform location. Rats in the HA group crossed the original platform location fewer times and spent less time in the target zone than rats in the control group (P<0.001). The decreases in the number of previous platform location crossings and time spent in the target area were more obvious in HR model rats than in control rats (P<0.001). In addition, compared to HA model rats, HR rats showed a significant decrease in the above two measures compared (P<0.01). These findings indicated that prolonged exposure to heroin can cause severe spatial memory impairment.

3. Analysis of axonal transport by MEMRI

3.1 Olfactory pathway structures

The structure of the nasal cavity and olfactory system of rats could be clearly observed by Mn^{2+}-enhanced T1W imaging (T1WI). A baseline image was obtained 6 h after administration of $MnCl_2$, and the SI in the OB on the ipsilateral side of the nasal cavity was significantly enhanced, indicating that Mn^{2+} was taken up in the turbinate and transported to olfactory sensory neurons in the OB. The structures of the OB, POT and DOT could be clearly observed in the MEMRI images taken at 24 h, as shown in Fig. 2.

3.2 SI of Mn^{2+} in the olfactory pathway

Enhancement of the Mn^{2+} signal in the OB and POT was observed in T1W images from AHE model rats taken at 6 h (compared with control rats P<0.001). At 6 h, the SI in the OB was not different between rats in the HA group and those in the control group (P>0.05), but the SI in the POT was higher in rats in the HA group than in control group rats (P<0.05). In HR model rats, an obvious reduction in the Mn^{2+} signal was observed in the OB (P<0.001), implying that the uptake of Mn^{2+} was decreased in these rats compared with control rats and that Mn^{2+} was not transported to the POT (P>0.05).

In the T1W images taken at 24 h, the SI in the OB, POT and DOT were significantly higher in AHE model rats than in control rats (P<0.001). The SI in the POT was increased (P<0.01), and the SI in the DOT was also higher in HA model rats than in control rats (P<0.05). The SIs in the OB, POT and DOT in HR model rats were significantly lower than those in control rats (P<0.001), as shown in Fig. 6.

3.3 ATR

In this study, the ATR, which was used to evaluate the effects of acute and prolonged exposure to heroin on axonal transport, was calculated from the change in the Mn^{2+} SI. The ATRs in the POT and DOT were increased in AHE model rats compared to control rats (P<0.001). The ATR of the POT was higher in HA model rats than in control rats (P<0.001), but the ATRs in the OB and DOT were not significantly different between HA model rats and control rats (P>0.05). The ATRs in the OB, POT and DOT were significantly lower in HR model rats than in control rats (P<0.001). The ATR in the OB in AHE model rats was increased

compared with that in HA model rats (P<0.01) and HR model rats (P<0.001). The ATR in the POT in AHE and HA model rats was higher than that in HR model rats (P<0.001). The ATR in the DOT in HR model rats was lower than that in AHE and HA model rats (P<0.001), as shown in Fig. 7. In general, AHE model rats showed the fastest axonal transport in the OB, POT and DOT, followed by HA model rats; in contrast, the ATR of HR model rats was the lowest, suggesting that axonal transport capacity was significantly reduced in HR model rats.

4. Western blotting

4.1 Expression of motor proteins involved in axonal transport

To study the effect of long-term heroin on axonal transport, the expression of kinesin-1 and cytoplasmic dynein, which have been found to play key roles in axonal transportation was assessed. The results showed that the level of KIF5 in rats in the HA group was not significantly different from that in rats in the control group (P>0.05) but that the level of cytoplasmic dynein was significantly decreased in rats in the HA group (P<0.01). In contrast, the expression levels of KIF5 and cytoplasmic dynein were significantly reduced in HR model rats (P<0.001, n=6 per group, Fig. 8).

4.2 Expression of proteins related to mitochondrial energy metabolism

COX IV and ATPB are the key enzymes in mitochondrial dynamics. ATPB levels were significantly reduced in HA model rats compared with rats in the control group (P<0.05), but there were no differences in COX IV expression between the HA group and control group (P>0.05). However, COX IV and ATPB levels in rats in the HR group were significantly lower than those in rats in the control group (P<0.001).

5. TEM

TEM was used to observe the ultrastructural changes in the brain after long-term exposure to heroin. Neurons undergoing apoptosis displayed nuclear condensation and mitochondrial swelling accompanied by mild demyelination in HR model rats. However, the morphology of synapses was normal, as shown in Fig. 9.

6. Immunofluorescence

We examined the cytoskeletal transport of NF-H, which is a neuron-specific cytoskeletal component, by immunostaining. NF-H is important for signal transmission along axons. As shown in Fig. 10, NF-H expression was significantly decreased in HR and HA model rats compared with control rats (n=6 per group, P<0.05).

7. Correlation analysis between the ATR and experimental indexes

Pearson's correlation was used to analyze the correlation of the ATR determined from MEMRI with MWM test data and protein expression. The results showed that the ATR was positively correlated with the number of previous platform location crossings and time spent in the target quadrant in the MWM test (r = 0.673, *P* = 0.008; r = 0.789, *P*=0.000). The expression of KIF5 and ATPB was positively correlated with the ATR (r = 0.54, *P* = 0.05; r = 0.699, *P* = 0.011).

Discussion

In this study, we investigated whether heroin administration affected axonal function and learning ability. We established rat models of heroin withdrawal at different periods for the first time; the model rats closely resembled heroin abusers in the clinic. Then, MEMRI was used to evaluate axonal transport in the HA and HR model rats and further explore the potential mechanism underlying changes in axonal transport. Our data showed that MEMRI can be used to evaluate axonal transport and that uptake and transport ability were decreased, spatial learning and memory were impaired, and brain ultrastructure was abnormal in rats experiencing long-term heroin relapsed.

Behavior and weight loss

Heroin acts on opioid receptors to form complexes or induce the release of endogenous opioids, which is believed to be the basis of mood changes(Kreek et al. 2012). In this study, rats exhibited increased excitability after injection of heroin and demonstrated withdrawal symptoms after naloxone administration. As the duration of drug abuse increased, withdrawal symptoms became more obvious, and the withdrawal score of HR model rats was higher than that of HA model rats. Klein et al(Klein et al. 2008) reported that the severity of withdrawal symptoms is related to the dose of heroin. Our results indicated that the influence of heroin on the behavior of rats was dose- and time-dependent. Additionally, heroin abuse can lead to weight loss in rats. In our study, the weight of rats in the HA and HR groups was lower than that of rats in the control group. These results are in agreement with previous observation(Li, Xia, Li, Yin, Wang, et al. 2017) and were probably caused by heroin-mediated activation of mu-opioid receptors in the intestinal wall and inhibition of pathways in the enteric nervous system, resulting in reduced peristalsis and slowed intestinal transit(Leppert 2015). Moreover, the weight loss of rats in the HR group was more pronounced, which may have been because long-term continuous addiction leads to more serious gastrointestinal damage.

Learning and memory deficits

Opioid addiction not only harms the gastrointestinal tract but also causes more serious damage to the CNS, which manifests as brain dysfunction, such as a decline in cognitive ability(Morie et al. 2015). Veschsanit reported that the administration of methamphetamine significantly impairs the learning ability of mice (Veschsanit et al. 2021). Morphine was also found to impair the spatial memory of mice in the Barnes maze test (Marks et al. 2021). In our study, the memory and learning ability of HA model rats

were decreased. Moreover, HA prolonged the escape latency and reduced the time spent in the previous platform quadrant and the number of previous platform location crossings, suggesting that heroin contributes to deficits in spatial learning and memory. The memory ability of heroin addicts is positively correlated with the time of drug use and dose of the drug, and the degree of memory impairment is correlated with the dose(Mitrović et al. 2011). Compared with rats with a short addiction stage, rats administered a higher dose of heroin and exposed to heroin for a prolonged period of time exhibited a longer escape latency, spent a shorter amount of time in the target quadrant, and made fewer entries into the target quadrant, implying that memory and learning ability were severely impaired in HR model rats. In addition, we found no difference in speed among any of the groups, which proves that the changes in behavior in the MWM test were not due to decreased activity.

Axonal transport deficits in rats exposed to heroin

As a highly fat-soluble substance, heroin can easily penetrate the blood–brain barrier (BBB) and cell membranes(Bao et al. 2007), leading to extensive nerve cell death and axonal degeneration. Heroin exposure caused learning and memory deficits in rats in the MWM test. However, the relationship between heroin-induced memory impairment and axonal function is not clear. We used MEMRI to evaluate axonal transport in the olfactory pathway in a heroin rat model. We calculated the ATR, which reflects axonal transport in vivo, by measuring the enhancement of the Mn^{2+} signal over time. Rats exposed to heroin for the first time showed significantly increased neuronal excitability and axonal transport, improved Mn^{2+} uptake in the OB, and an increased ATR in the OB, POT and DOT. Aimino et al (Aimino et al. 2018) found that in acute alcoholism, large amounts of alcohol increases the release of presynaptic neurotransmitters in neurons and neuronal excitability. Axonal transport decreased with short term heroin exposures compared with the first heroin exposure, but neurons remained in an excited state. Axonal transport in POT and DOT was decreased in HA model rats compared with AHE model rats but was higher in HA model rats than rats in the control group. Importantly, axonal damage can lead to a decrease in Mn^{2+} uptake, resulting in a decrease in SI(Minoshima et al. 2008; Sharma et al. 2010). Furthermore, long-term heroin relapsed and withdrawal disrupt axonal transport. The enhancement of the Mn^{2+} signal in the OB was significantly decreased in HR model rats, suggesting that Mn^{2+} uptake ability was reduced in the OB. The ATRs in the OB, POT and DOT in HR model rats were significantly decreased and lower than those in HA model rats, which indicated that the impairment of axonal transport was further aggravated as the duration of HA increased. Overall, MEMRI can be used to dynamically monitor the effect of drug addiction on axonal transport.

Mechanism underlying the decrease in axonal transport

To further elucidate the mechanism underlying the decline in axonal transport after long-term exposure to heroin, we analyzed it from the perspective of axonal transport dynamics and energy metabolism. Axonal transport is mediated by two types of adenosine triphosphate (ATP)-dependent motors, i.e., kinesin and

cytoplasmic dynein, which use microtubules for transport(Gibbs et al. 2015). KIF5 belongs to the kinesin family and is responsible for transporting various cargos in mammalian neurons (Karle et al. 2012; Morfini et al. 2016). Cytoplasmic dynein is the main motor that drives retrograde transport (Maday et al. 2014). Naughton reported(Naughton et al. 2018) that diisopropylfluorophosphate exposure causes axonal transport impairment by decreasing cytoplasmic dynein levels. In HA model rats, the level of KIF5 did not change, but the level of cytoplasmic dynein decreased. This may have been because short-term use of heroin did not have a marked impact on axonal transport. In HR model rats, the levels of KIF5 and cytoplasmic dynein were significantly reduced, which indicated that axonal transport was impaired. Previous studies have indicated that destruction of the kinesin transport system reduces the rate of Mn^{2+} transport in the optic nerve(Bearer et al. 2007). Our MEMRI results showed that the ATR was the most markedly altered in the HR group, suggesting that long-term repeated heroin abuse destroys the key regulatory factors of axonal transport, leading to axonal transport dysfunction.

We further studied the changes in mitochondrial energy metabolism involved in axonal transport. Axonal transport relies on energy generated by ATP (Middlemore-Risher et al. 2011). Mitochondria are the main organelles that produce energy, and mitochondrial destruction reduces the production of ATP, leading to impaired axonal transport(Akbari et al. 2019; Zinsmaier et al. 2009). ATP synthase and COX IV are key enzymes for supplying energy to the cell (Fernandez et al. 2019; Morelli et al. 2020). COX IV is a nuclear-encoded mitochondrial protein that plays an essential role in oxidative phosphorylation and axonal function(Aschrafi et al. 2012). Aschrafi et al (Aschrafi et al. 2010) reported that inhibition of COX IV expression significantly decreases axonal transmission capacity. Our data showed that the ATPB level in HA model rats was lower than that in rats in the control group, while COX IV expression showed no significant change. However, in HR model rats, the levels of ATPB and COX IV were significantly reduced. These results indicate that continuous withdrawal and relapse of heroin can cause mitochondrial dysfunction and affect axons. This was also confirmed by TEM, as mitochondrial swelling and neuronal apoptosis were observed in HR model rats. Further analysis of the correlation between the ATR and protein expression showed that the ATR was positively correlated with the expression levels of ATPB and KIF5, indicating that the decrease in axonal transport in rats was inevitably related to the function of axons and mitochondria and suggesting that HA and HR had a gradual effect on the CNS, which may have been related to the dose of heroin and duration of heroin exposure.

In addition, neurofilaments are the structural components of axons and synapses and are essential for the transmission of electrical signals along axons(Lee et al. 2020). The NF-H level was decreased in HA and HR model rats, implying that heroin also damaged the axon cytoskeleton, resulting in slow axonal transport.

Conclusions

We used MEMRI to evaluate axonal transport in heroin models after different withdrawal periods. Long-term heroin withdrawal impairs axonal transport and induces learning and memory deficits; these

changes may be related to a reduction in the levels of motor proteins and mitochondrial dysfunction. The findings provide new insights into methods for evaluating axonal transport for the study of addiction.

Declarations

Authors contributions

Yueyuan Luo:Performed the experiments, data interpretation, wrote the manuscript. Chengde Liao, Long Chen and Qinqing Li:Edited the manuscript. Yongjin Zhang, Shasha Bao, Ailin Deng and Tengfei Ke: Performed the experiments, data interpretation,MRI scan and analysis. Jun Yang: Study design, data interpretation, edited the manuscript.

All authors read and approved the final manuscript.

Funding information

This study was supported by the NHC Key Laboratory of Drug Addiction Medicine (2020DAMARB-005), the National Natural Science Foundation of China (grant no. 82060313, 81703155, 81960496, 82160340), the Yunnan Health Training Project of High Level Talents (H-2017005, D-2018009, H-2018006), Yunnan Province education department scientific research fund (2021Y342,2019J1280) and the Yunnan Applied Basic Research Projects-KMMU Joint Special Project (202001AY070001-072)

Informed consent

This study did not involve informed consent obtained by individuals.

Data and materials availability

The datasets generated and analyzed during the current study are available from the corresponding author on request.

Ethical approval

The animal experiments were conducted in accordance with the standard guidelines of the Institutional Animal Care and Experiment Committee of Kunming Medical University（KMMU2020356）.

Consent to participate

Not applicable.

Consent to publish

Not applicable.

Competing interests

The authors declare that they have no conflict of interest.

References

1. Aimino, M. A., Coker, C. R., & Silberman, Y. (2018). Acute ethanol modulation of neurocircuit function in the nucleus of the tractus solitarius. *Brain Res Bull, 138*, 5-11.http://doi.org/10.1016/j.brainresbull.2017.07.019
2. Akbari, M., Kirkwood, T. B. L., & Bohr, V. A. (2019). Mitochondria in the signaling pathways that control longevity and health span. *Ageing Res Rev, 54*, 100940.http://doi.org/10.1016/j.arr.2019.100940
3. Almeida-Corrêa, S., Czisch, M., & Wotjak, C. T. (2018). In Vivo Visualization of Active Polysynaptic Circuits With Longitudinal Manganese-Enhanced MRI (MEMRI). *Front Neural Circuits, 12*, 42.http://doi.org/10.3389/fncir.2018.00042
4. Anthony, I. C., Norrby, K. E., Dingwall, T., Carnie, F. W., Millar, T., Arango, J. C., . . . Bell, J. E. (2010). Predisposition to accelerated Alzheimer-related changes in the brains of human immunodeficiency virus negative opiate abusers. *Brain, 133*(Pt 12), 3685-3698.http://doi.org/10.1093/brain/awq263
5. Aschrafi, A., Kar, A. N., Natera-Naranjo, O., MacGibeny, M. A., Gioio, A. E., & Kaplan, B. B. (2012). MicroRNA-338 regulates the axonal expression of multiple nuclear-encoded mitochondrial mRNAs encoding subunits of the oxidative phosphorylation machinery. *Cell Mol Life Sci, 69*(23), 4017-4027.http://doi.org/10.1007/s00018-012-1064-8
6. Aschrafi, A., Natera-Naranjo, O., Gioio, A. E., & Kaplan, B. B. (2010). Regulation of axonal trafficking of cytochrome c oxidase IV mRNA. *Mol Cell Neurosci, 43*(4), 422-430.http://doi.org/10.1016/j.mcn.2010.01.009
7. Bao, G., Kang, L., Li, H., Li, Y., Pu, L., Xia, P., . . . Pei, G. (2007). Morphine and heroin differentially modulate in vivo hippocampal LTP in opiate-dependent rat. *Neuropsychopharmacology, 32*(8), 1738-1749.http://doi.org/10.1038/sj.npp.1301308
8. Barnett, M. H., Miller, L. A., Reddel, S. W., & Davies, L. (2001). Reversible delayed leukoencephalopathy following intravenous heroin overdose. *J Clin Neurosci, 8*(2), 165-167.http://doi.org/10.1054/jocn.2000.0769
9. Barnhart, C. D., Yang, D., & Lein, P. J. (2015). Using the Morris water maze to assess spatial learning and memory in weanling mice. *PLoS One, 10*(4), e0124521.http://doi.org/10.1371/journal.pone.0124521

10. Bassiony, M. M., Youssef, U. M., Hassan, M. S., Salah El-Deen, G. M., El-Gohari, H., Abdelghani, M., . . . Ibrahim, D. H. (2017). Cognitive Impairment and Tramadol Dependence. *J Clin Psychopharmacol, 37*(1), 61-66.http://doi.org/10.1097/jcp.0000000000000617
11. Bearer, E. L., Falzone, T. L., Zhang, X., Biris, O., Rasin, A., & Jacobs, R. E. (2007). Role of neuronal activity and kinesin on tract tracing by manganese-enhanced MRI (MEMRI). *Neuroimage, 37 Suppl 1*(Suppl 1), S37-46.http://doi.org/10.1016/j.neuroimage.2007.04.053
12. Bora, E., Yücel, M., Fornito, A., Pantelis, C., Harrison, B. J., Cocchi, L., . . . Lubman, D. I. (2012). White matter microstructure in opiate addiction. *Addict Biol, 17*(1), 141-148.http://doi.org/10.1111/j.1369-1600.2010.00266.x
13. Büttner, A., Mall, G., Penning, R., & Weis, S. (2000). The neuropathology of heroin abuse. *Forensic Sci Int, 113*(1-3), 435-442.http://doi.org/10.1016/s0379-0738(00)00204-8
14. Büttner, A., Rohrmoser, K., Mall, G., Penning, R., & Weis, S. (2006). Widespread axonal damage in the brain of drug abusers as evidenced by accumulation of beta-amyloid precursor protein (beta-APP): an immunohistochemical investigation. *Addiction, 101*(9), 1339-1346.http://doi.org/10.1111/j.1360-0443.2006.01505.x
15. Cadet, J. L., Bisagno, V., & Milroy, C. M. (2014). Neuropathology of substance use disorders. *Acta Neuropathol, 127*(1), 91-107.http://doi.org/10.1007/s00401-013-1221-7
16. Deng, W., Faiq, M. A., Liu, C., Adi, V., & Chan, K. C. (2019). Applications of Manganese-Enhanced Magnetic Resonance Imaging in Ophthalmology and Visual Neuroscience. *Front Neural Circuits, 13*, 35.http://doi.org/10.3389/fncir.2019.00035
17. Fernandez, A., Meechan, D. W., Karpinski, B. A., Paronett, E. M., Bryan, C. A., Rutz, H. L., . . . LaMantia, A. S. (2019). Mitochondrial Dysfunction Leads to Cortical Under-Connectivity and Cognitive Impairment. *Neuron, 102*(6), 1127-1142.e1123.http://doi.org/10.1016/j.neuron.2019.04.013
18. Fitzpatrick, R. E., Rubenis, A. J., Lubman, D. I., & Verdejo-Garcia, A. (2020). Cognitive deficits in methamphetamine addiction: Independent contributions of dependence and intelligence. *Drug Alcohol Depend, 209*, 107891.http://doi.org/10.1016/j.drugalcdep.2020.107891
19. Gardini, S., & Venneri, A. (2012). Reduced grey matter in the posterior insula as a structural vulnerability or diathesis to addiction. *Brain Res Bull, 87*(2-3), 205-211.http://doi.org/10.1016/j.brainresbull.2011.11.021
20. Gibbs, K. L., Greensmith, L., & Schiavo, G. (2015). Regulation of Axonal Transport by Protein Kinases. *Trends Biochem Sci, 40*(10), 597-610.http://doi.org/10.1016/j.tibs.2015.08.003
21. Gruber, S. A., Silveri, M. M., & Yurgelun-Todd, D. A. (2007). Neuropsychological consequences of opiate use. *Neuropsychol Rev, 17*(3), 299-315.http://doi.org/10.1007/s11065-007-9041-y
22. Guo, T., Noble, W., & Hanger, D. P. (2017). Roles of tau protein in health and disease. *Acta Neuropathol, 133*(5), 665-704.http://doi.org/10.1007/s00401-017-1707-9
23. Guo, W., Stoklund Dittlau, K., & Van Den Bosch, L. (2020). Axonal transport defects and neurodegeneration: Molecular mechanisms and therapeutic implications. *Semin Cell Dev Biol, 99*, 133-150.http://doi.org/10.1016/j.semcdb.2019.07.010

24. Karle, K. N., Möckel, D., Reid, E., & Schöls, L. (2012). Axonal transport deficit in a KIF5A(-/-) mouse model. *Neurogenetics, 13*(2), 169-179.http://doi.org/10.1007/s10048-012-0324-y
25. Kashyap, S., Majeed, G., Bowen, I., Beamer, Y., & Miulli, D. (2020). Toxic Leukoencephalopathy due to Inhalational Heroin Abuse. *Ann Indian Acad Neurol, 23*(4), 542-544.http://doi.org/10.4103/aian.AIAN_446_18
26. Klein, G., Juni, A., Arout, C. A., Waxman, A. R., Inturrisi, C. E., & Kest, B. (2008). Acute and chronic heroin dependence in mice: contribution of opioid and excitatory amino acid receptors. *Eur J Pharmacol, 586*(1-3), 179-188.http://doi.org/10.1016/j.ejphar.2008.02.035
27. Kousik, S. M., Carvey, P. M., & Napier, T. C. (2014). Methamphetamine self-administration results in persistent dopaminergic pathology: implications for Parkinson's disease risk and reward-seeking. *Eur J Neurosci, 40*(4), 2707-2714.http://doi.org/10.1111/ejn.12628
28. Kreek, M. J., Levran, O., Reed, B., Schlussman, S. D., Zhou, Y., & Butelman, E. R. (2012). Opiate addiction and cocaine addiction: underlying molecular neurobiology and genetics. *J Clin Invest, 122*(10), 3387-3393.http://doi.org/10.1172/jci60390
29. Kumar, N., Bhalla, M. C., Frey, J. A., & Southern, A. (2015). Intraparenchymal hemorrhage after heroin use. *Am J Emerg Med, 33*(8), 1109.e1103-1104.http://doi.org/10.1016/j.ajem.2015.01.007
30. Lee, Y., Lee, B. H., Yip, W., Chou, P., & Yip, B. S. (2020). Neurofilament Proteins as Prognostic Biomarkers in Neurological Disorders. *Curr Pharm Des, 25*(43), 4560-4569.http://doi.org/10.2174/1381612825666191210154535
31. Leppert, W. (2015). Emerging therapies for patients with symptoms of opioid-induced bowel dysfunction. *Drug Des Devel Ther, 9*, 2215-2231.http://doi.org/10.2147/dddt.S32684
32. Li, Y., Xia, B., Li, R., Yin, D., & Liang, W. (2017). Changes in Expression of Dopamine, Its Receptor, and Transporter in Nucleus Accumbens of Heroin-Addicted Rats with Brain-Derived Neurotrophic Factor (BDNF) Overexpression. *Med Sci Monit, 23*, 2805-2815.http://doi.org/10.12659/msm.904670
33. Li, Y., Xia, B., Li, R., Yin, D., Wang, Y., & Liang, W. (2017). Expression of brain-derived neurotrophic factors, neurotrophin-3, and neurotrophin-4 in the nucleus accumbens during heroin dependency and withdrawal. *Neuroreport, 28*(11), 654-660.http://doi.org/10.1097/wnr.0000000000000810
34. Lin, Y. J., & Koretsky, A. P. (1997). Manganese ion enhances T1-weighted MRI during brain activation: an approach to direct imaging of brain function. *Magn Reson Med, 38*(3), 378-388.http://doi.org/10.1002/mrm.1910380305
35. Lwin, T., Yang, J. L., Ngampramuan, S., Viwatpinyo, K., Chancharoen, P., Veschsanit, N., . . . Mukda, S. (2021). Melatonin ameliorates methamphetamine-induced cognitive impairments by inhibiting neuroinflammation via suppression of the TLR4/MyD88/NFκB signaling pathway in the mouse hippocampus. *Prog Neuropsychopharmacol Biol Psychiatry, 111*, 110109.http://doi.org/10.1016/j.pnpbp.2020.110109
36. Ma, X., Qiu, Y., Tian, J., Wang, J., Li, S., Zhan, W., . . . Xu, Y. (2015). Aberrant default-mode functional and structural connectivity in heroin-dependent individuals. *PLoS One, 10*(4), e0120861.http://doi.org/10.1371/journal.pone.0120861

37. Maday, S., Twelvetrees, A. E., Moughamian, A. J., & Holzbaur, E. L. (2014). Axonal transport: cargo-specific mechanisms of motility and regulation. *Neuron, 84*(2), 292-309.http://doi.org/10.1016/j.neuron.2014.10.019

38. Mandal, A., & Drerup, C. M. (2019). Axonal Transport and Mitochondrial Function in Neurons. *Front Cell Neurosci, 13*, 373.http://doi.org/10.3389/fncel.2019.00373

39. Marks, W. D., Paris, J. J., Barbour, A. J., Moon, J., Carpenter, V. J., McLane, V. D., . . . Hauser, K. F. (2021). HIV-1 Tat and Morphine Differentially Disrupt Pyramidal Cell Structure and Function and Spatial Learning in Hippocampal Area CA1: Continuous versus Interrupted Morphine Exposure. *eNeuro, 8*(3).http://doi.org/10.1523/eneuro.0547-20.2021

40. Martínez-Mármol, R., Mohannak, N., Qian, L., Wang, T., Gormal, R. S., Ruitenberg, M. J., . . . Meunier, F. A. (2019). p110δ PI3-Kinase Inhibition Perturbs APP and TNFα Trafficking, Reduces Plaque Burden, Dampens Neuroinflammation, and Prevents Cognitive Decline in an Alzheimer's Disease Mouse Model. *J Neurosci, 39*(40), 7976-7991.http://doi.org/10.1523/jneurosci.0674-19.2019

41. Middlemore-Risher, M. L., Adam, B. L., Lambert, N. A., & Terry, A. V., Jr. (2011). Effects of chlorpyrifos and chlorpyrifos-oxon on the dynamics and movement of mitochondria in rat cortical neurons. *J Pharmacol Exp Ther, 339*(2), 341-349.http://doi.org/10.1124/jpet.111.184762

42. Minoshima, S., & Cross, D. (2008). In vivo imaging of axonal transport using MRI: aging and Alzheimer's disease. *Eur J Nucl Med Mol Imaging, 35 Suppl 1*, S89-92.http://doi.org/10.1007/s00259-007-0707-8

43. Mitrović, S. M., Dickov, A., Vučković, N., Mitrović, D., & Budiša, D. (2011). The effect of heroin on verbal memory. *Psychiatr Danub, 23*(1), 53-59

44. Morelli, A. M., Ravera, S., & Panfoli, I. (2020). The aerobic mitochondrial ATP synthesis from a comprehensive point of view. *Open Biol, 10*(10), 200224.http://doi.org/10.1098/rsob.200224

45. Morfini, G., Schmidt, N., Weissmann, C., Pigino, G., & Kins, S. (2016). Conventional kinesin: Biochemical heterogeneity and functional implications in health and disease. *Brain Res Bull, 126*(Pt 3), 347-353.http://doi.org/10.1016/j.brainresbull.2016.06.009

46. Morie, K. P., Nich, C., Hunkele, K., Potenza, M. N., & Carroll, K. M. (2015). Alexithymia level and response to computer-based training in cognitive behavioral therapy among cocaine-dependent methadone maintained individuals. *Drug Alcohol Depend, 152*, 157-163.http://doi.org/10.1016/j.drugalcdep.2015.04.004

47. Naughton, S. X., Hernandez, C. M., Beck, W. D., Poddar, I., Yanasak, N., Lin, P. C., & Terry, A. V., Jr. (2018). Repeated exposures to diisopropylfluorophosphate result in structural disruptions of myelinated axons and persistent impairments of axonal transport in the brains of rats. *Toxicology, 406-407*, 92-103.http://doi.org/10.1016/j.tox.2018.06.004

48. Ornstein, T. J., Iddon, J. L., Baldacchino, A. M., Sahakian, B. J., London, M., Everitt, B. J., & Robbins, T. W. (2000). Profiles of cognitive dysfunction in chronic amphetamine and heroin abusers. *Neuropsychopharmacology, 23*(2), 113-126.http://doi.org/10.1016/s0893-133x(00)00097-x

49. Pautler, R. G., Silva, A. C., & Koretsky, A. P. (1998). In vivo neuronal tract tracing using manganese-enhanced magnetic resonance imaging. *Magn Reson Med, 40*(5), 740-748.http://doi.org/10.1002/mrm.1910400515
50. Potvin, S., Pelletier, J., Grot, S., Hébert, C., Barr, A. M., & Lecomte, T. (2018). Cognitive deficits in individuals with methamphetamine use disorder: A meta-analysis. *Addict Behav, 80*, 154-160.http://doi.org/10.1016/j.addbeh.2018.01.021
51. Pu, H., Wang, X., Zhang, J., Ma, C., Su, Y., Li, X., . . . Su, L. (2015). Cerebellar neuronal apoptosis in heroin-addicted rats and its molecular mechanism. *Int J Clin Exp Pathol, 8*(7), 8260-8267
52. Sau, D., Rusmini, P., Crippa, V., Onesto, E., Bolzoni, E., Ratti, A., & Poletti, A. (2011). Dysregulation of axonal transport and motorneuron diseases. *Biol Cell, 103*(2), 87-107.http://doi.org/10.1042/bc20100093
53. Sempere, A. P., Posada, I., Ramo, C., & Cabello, A. (1991). Spongiform leucoencephalopathy after inhaling heroin. *Lancet, 338*(8762), 320.http://doi.org/10.1016/0140-6736(91)90463-y
54. Sharma, R., Buras, E., Terashima, T., Serrano, F., Massaad, C. A., Hu, L., . . . Pautler, R. G. (2010). Hyperglycemia induces oxidative stress and impairs axonal transport rates in mice. *PLoS One, 5*(10), e13463.http://doi.org/10.1371/journal.pone.0013463
55. Silva, A. C., & Bock, N. A. (2008). Manganese-enhanced MRI: an exceptional tool in translational neuroimaging. *Schizophr Bull, 34*(4), 595-604.http://doi.org/10.1093/schbul/sbn056
56. Uselman, T. W., Barto, D. R., Jacobs, R. E., & Bearer, E. L. (2020). Evolution of brain-wide activity in the awake behaving mouse after acute fear by longitudinal manganese-enhanced MRI. *Neuroimage, 222*, 116975.http://doi.org/10.1016/j.neuroimage.2020.116975
57. Veschsanit, N., Yang, J. L., Ngampramuan, S., Viwatpinyo, K., Pinyomahakul, J., Lwin, T., . . . Mukda, S. (2021). Melatonin reverts methamphetamine-induced learning and memory impairments and hippocampal alterations in mice. *Life Sci, 265*, 118844.http://doi.org/10.1016/j.lfs.2020.118844
58. Wu, X., Pang, G., Zhang, Y. M., Li, G., Xu, S., Dong, L., . . . Zhang, G. (2015). Activation of serotonin 5-HT(2C) receptor suppresses behavioral sensitization and naloxone-precipitated withdrawal symptoms in heroin-treated mice. *Neurosci Lett, 607*, 23-28.http://doi.org/10.1016/j.neulet.2015.09.013
59. Yang, J., Li, Q., Han, D., Liao, C., Wang, P., Gao, J., . . . Liu, Y. (2020). Radiation-induced impairment of optic nerve axonal transport in tree shrews and rats monitored by longitudinal manganese-enhanced MRI. *Neurotoxicology, 77*, 145-154.http://doi.org/10.1016/j.neuro.2020.01.008
60. Zinsmaier, K. E., Babic, M., & Russo, G. J. (2009). Mitochondrial transport dynamics in axons and dendrites. *Results Probl Cell Differ, 48*, 107-139.http://doi.org/10.1007/400_2009_20

Figures

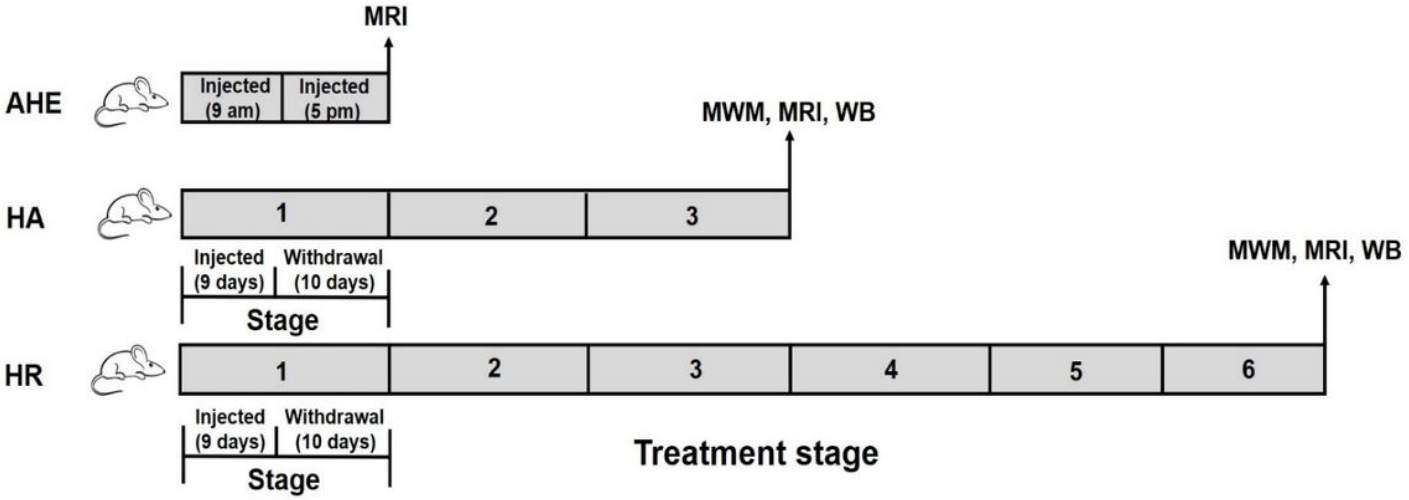

Figure 1

A schematic diagram of the schedule used to construct the animal models. Each stage involved 9 consecutive days of heroin injection and 10 days of spontaneous withdrawal. AHE indicates rats that received only two injections (at 9 am and 5 pm). HA indicates rats that underwent three stages of heroin treatment. HR indicates rats that underwent six stages of treatment.

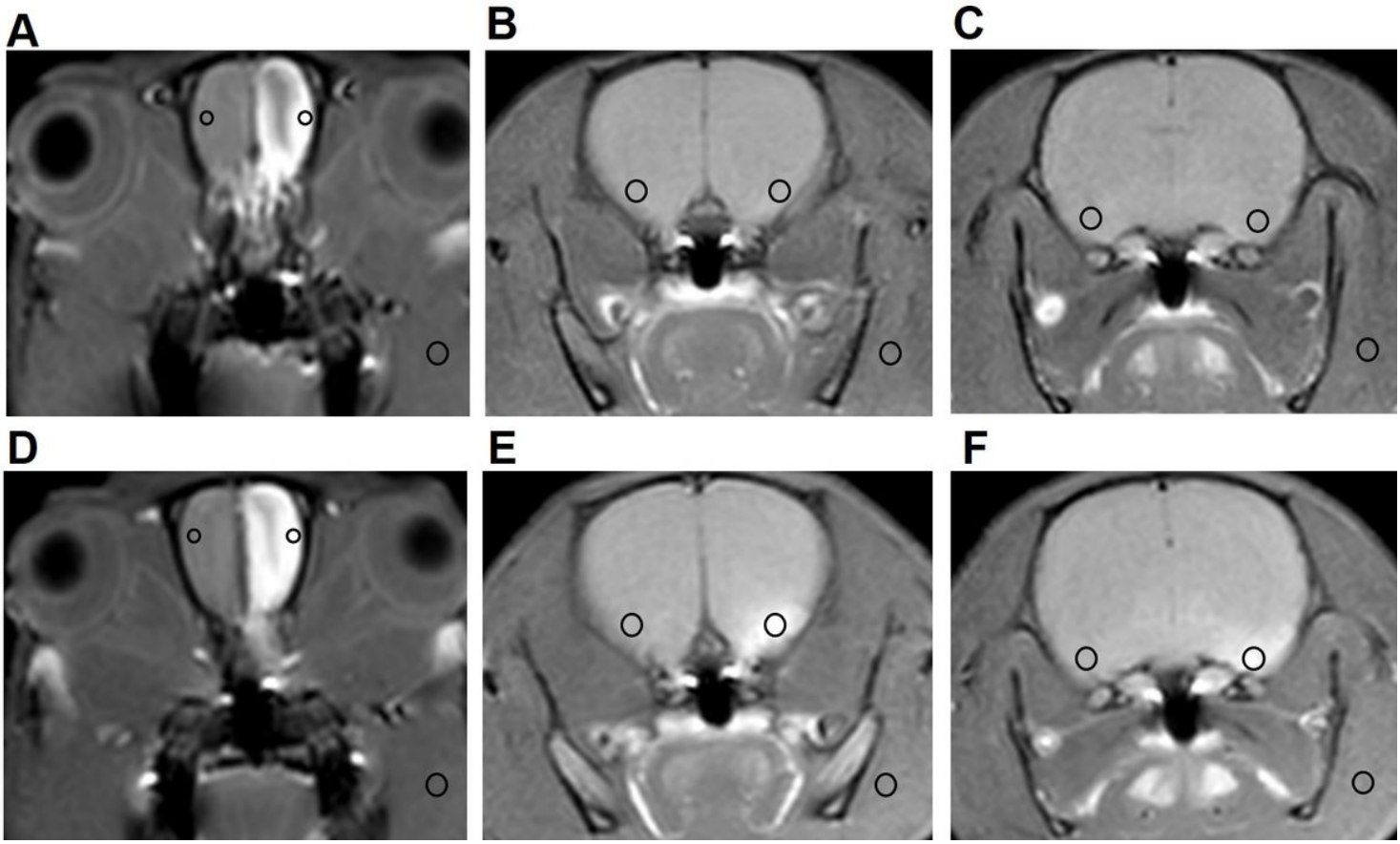

Figure 2

Visualization of the olfactory pathways of rats by MEMRI. Mn^{2+}-enhanced imaging of olfactory pathways at 6 h (A-C) and 24 h (D-F). Mn^{2+}-enhanced images of (A) the OB, (B) the POT, and (C) the DOT. The circles on the images of the olfactory system represent the regions of interest (ROIs), i.e., the regions in which the SI was measured. OB: olfactory bulb; POT: proximal olfactory tract; DOT: distal olfactory tract.

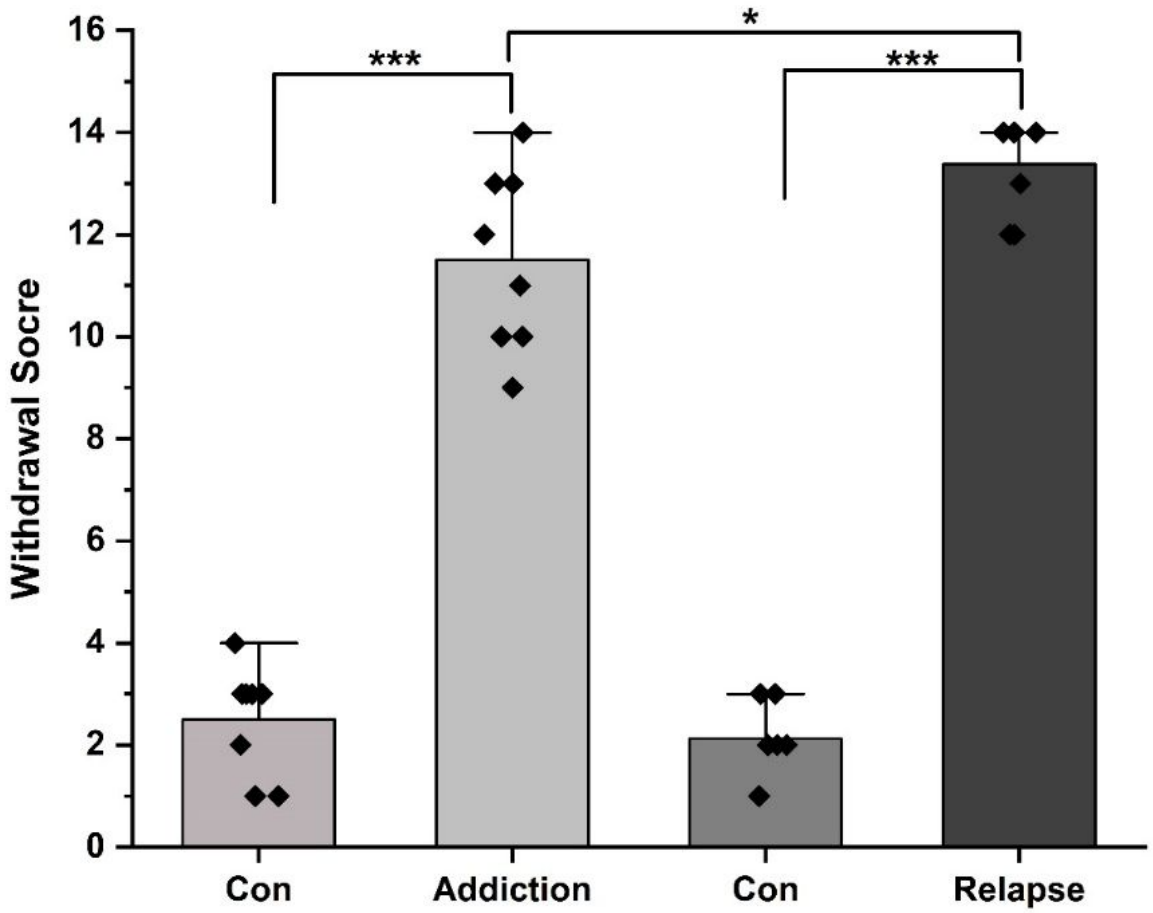

Figure 3

Withdrawal scores of the different groups. The score of rats in the HA group was 12.16±1.47 and that of rats in the HR group was 13.66±0.81 (*** $P < 0.001$ and * $P < 0.05$ compared with rats in the control group). Con: control group; Addiction: HA group; Relapse: HR group.

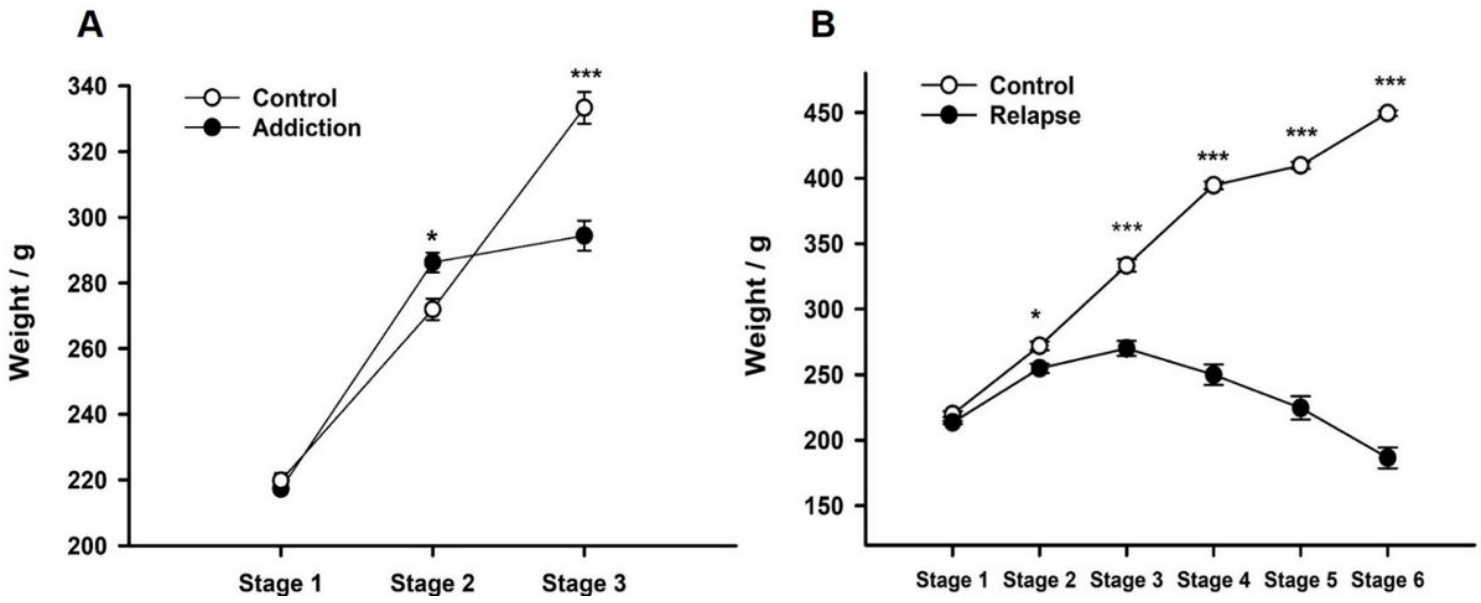

Figure 4

Body weight of rats in each stage. The data are presented as the mean ± SEM. Significant differences are indicated by *$P < 0.05$ and ***$P < 0.001$ (compared with rats in the control group). Addiction: HA group; Relapse: HR group.

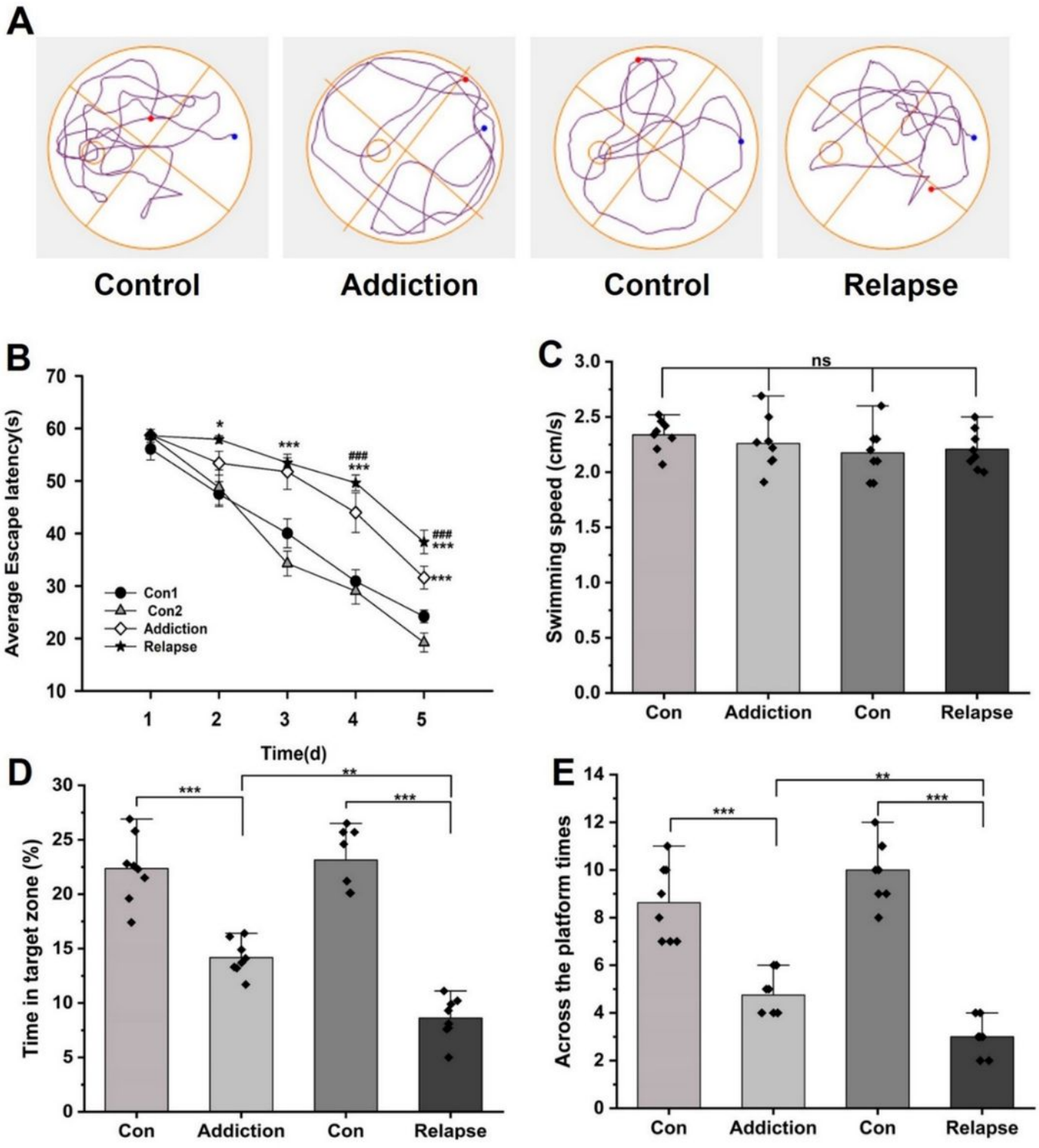

Figure 5

The effect of heroin on the learning and memory ability of rats in the MWM test. In the navigation test of the MWM test, the escape latency of rats exposed to heroin was longer than that of rats in the control group (B). Swimming speed was not significantly different among any of the groups (C). In the probe test, the swimming trajectories of the rats after removal of the platform revealed that the number and percentage in the heroin treatment group that passed times through the original platform quadrant were

reduced (A). The time spent in the target zone (D) and the number of previous platform location crossings (E) were used to evaluate the memory of the rats. The data are expressed as the mean ± SEM (n = 10). Significant differences in escape latency are indicated by *P < 0.05, **P < 0.01, and ***P < 0.001; # indicates a significant different between HR model rats and HA model rats (###P<0.001). ns indicates no significant difference between the two groups. Con: control group; Addiction: HA group; Relapse: HR group.

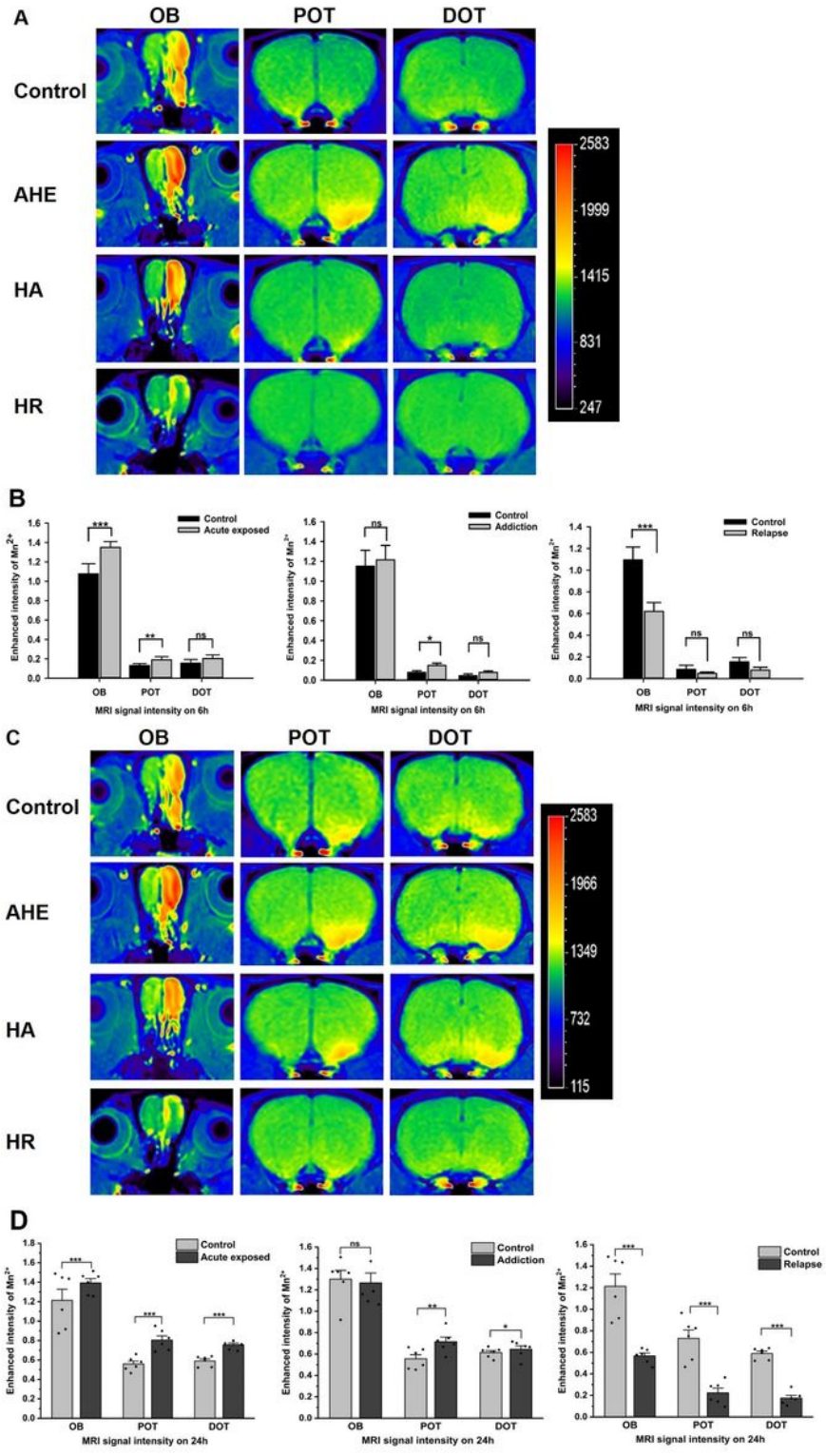

Figure 6

Mn^{2+}-enhanced T1WI and quantification of the SI in AHE, HA and HR model rats. Coronal T1W images of rats 6 h (A) and 24 h (C) after $MnCl_2$ injection. Quantitative analyses of the Mn^{2+} SI 6 h (B) and 24 h (D) after injection of Mn^{2+} solution. (B) Enhancement of the Mn^{2+} signal in the OB and POT was observed in AHE model rats, and the SI in the POT was higher in HA model rats. In HR model rats, a reduction in the SI was observed in the OB. (D) The SI in the OB, POT and DOT were higher in AHE model rats, and the SI in the DOT and POT were increased in HA model rats. In HR model rats, the SI in the OB, POT and DOT were significantly lower. The data are presented as the mean ± SEM. * P<0.05, ** P<0.01, and *** P<0.001; ns indicates no significant difference between the two groups. OB: olfactory bulb, POT: proximal olfactory tract, DOT: distal olfactory tract.

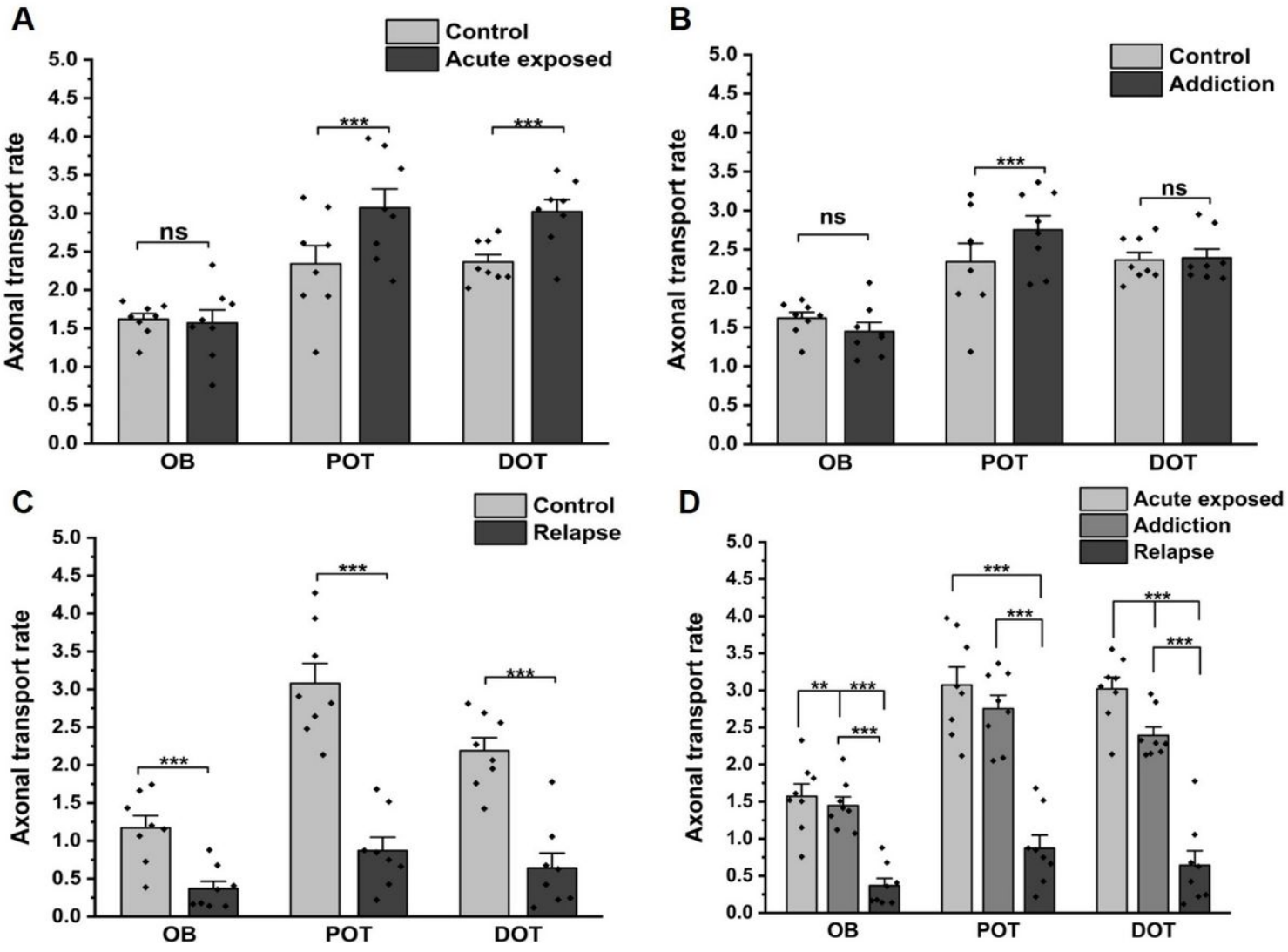

Figure 7

Quantification of the ATR of Mn^{2+} in AHE, HA and HR model rats.

The ATR in the OB, POT and DOT were the lowest in HR model rats, and AHE model rats exhibited the fastest axonal transport, followed by HA model rats. (A) The ATR in POT and DOT were increased in AHE model rats. (B) The ATR in the POT in the HA group was higher than that in the control group. (C) The ATR in the OB, POT and DOT were decreased in the HR group. (D) The ATR of the HR group was lower than that of the AHE and HA groups. The data are presented as the mean ± SEM. * P <0.05, ** P <0.01, and *** P <0.001; ns indicates no significant difference between the two groups.

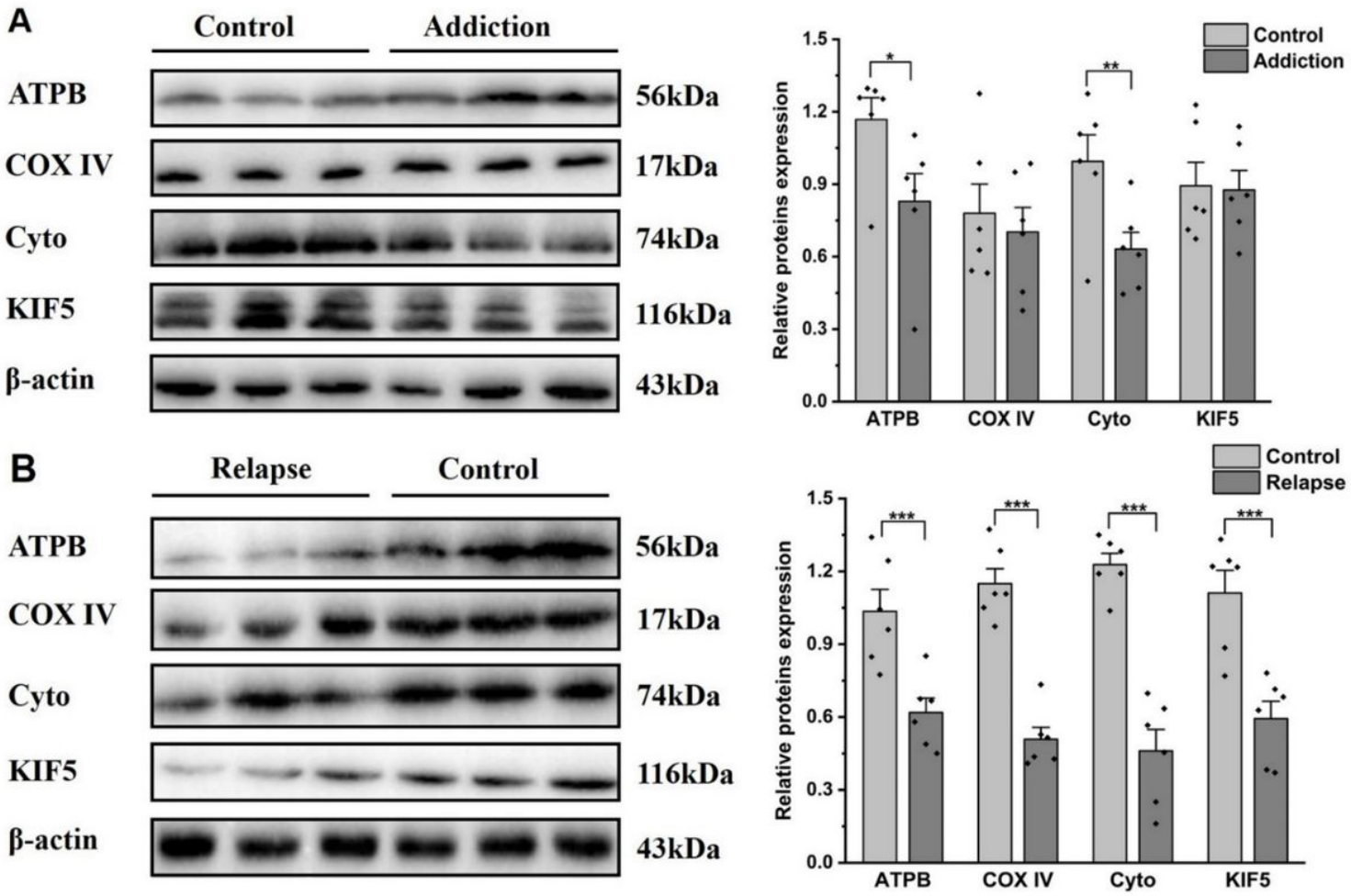

Figure 8

The expression levels of axonal motor proteins and energy metabolism-related proteins. (A) The protein expression levels of ATPB and cytoplasmic dynein were reduced in HA model rats. (B) ATPB, COX IV, cytoplasmic dynein and KIF5 protein levels were decreased in HR model rats. Each bar represents the mean±SEM (n=6), and significant differences in expression are indicated by *P < 0.05, **P < 0.01, and ***P < 0.001.

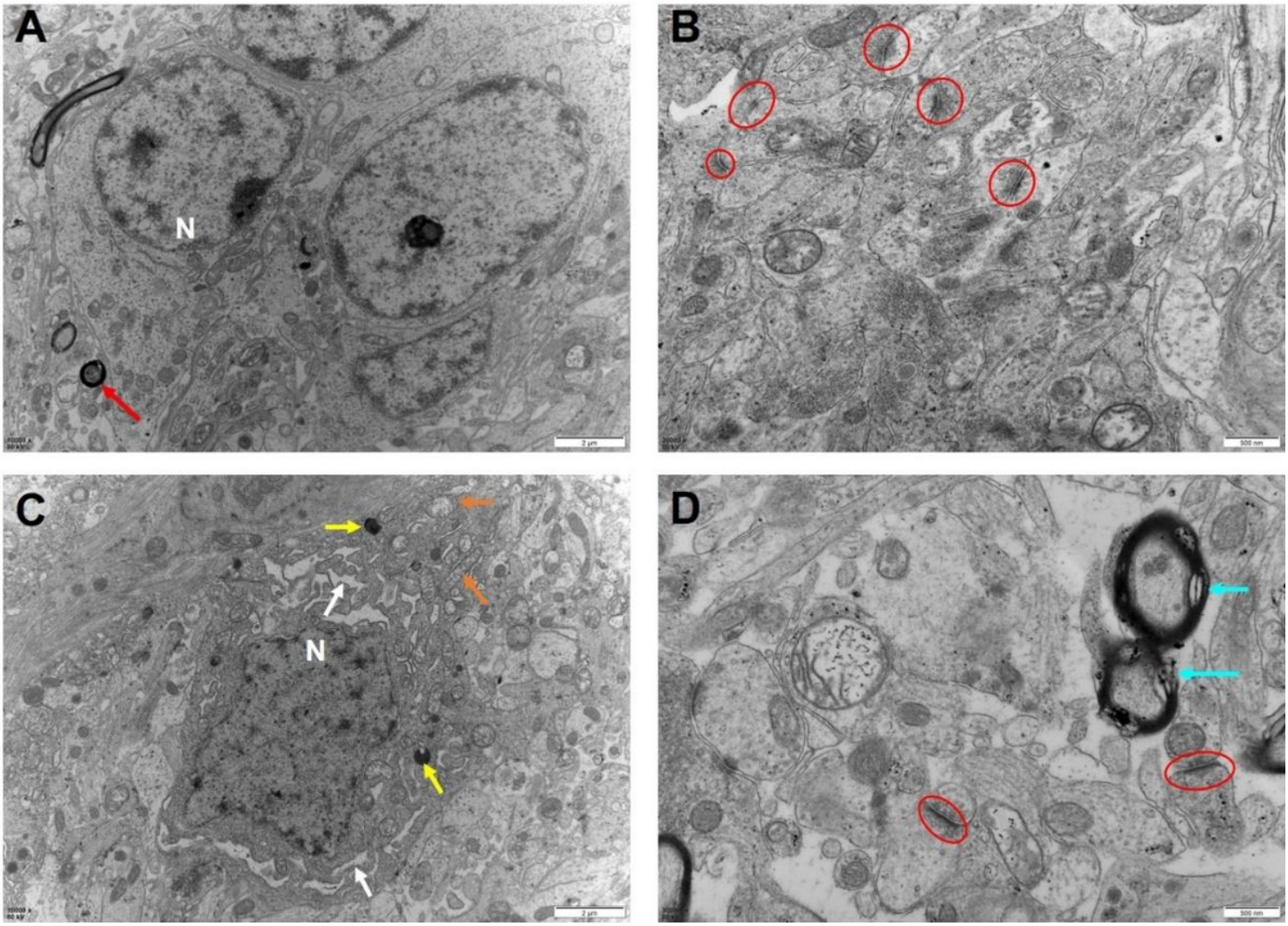

Figure 9

Ultrastructure of neurons and axons in rats in the control group (A and B) and HR model rats (C and D). In the image of neurons with a normal structure, the red arrow indicates normal myelinated nerve fibers (A). The objects marked by the red circles are normal synaptic structures (B). Neuronal cell apoptosis was observed, mitochondria were swollen (orange arrows), and the rough endoplasmic reticulum was expanded (white arrows), with secondary lysosomes (yellow arrows) (C). Demyelination of nerve fibers (blue arrows) is shown (D). N: neurons.

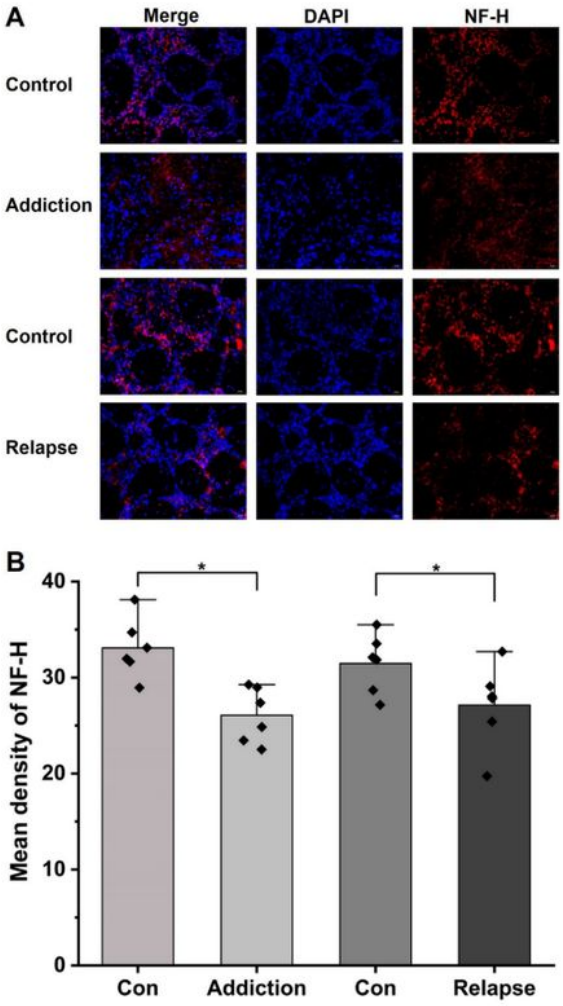

Figure 10

Immunofluorescence staining of NF-H in the OB. The staining intensity was significantly reduced in HA and HR model rats. The data are presented as the mean ± SEM. Significant differences are indicated by *$P < 0.05$. Con: control group; Addiction: HA group; Relapse: HR group.

Supplementary Files

This is a list of supplementary files associated with this preprint. Click to download.

- AuthorChecklist.pdf